

Thermo-electrochemical reduction of sulfate to sulfide using a graphite cathode

B. A. BILAL, H. TRIBUTSCH

Hahn Meitner Institut Berlin, Dep. Solare Energetik, Glienicker Straße 100, 14109 Berlin, Germany

Received 18 August 1997; accepted in revised form 29 January 1998

A thermoelectrochemical process which allows reduction of sulfate to sulfide with current efficiency of 80% using graphitic carbon as an electrode is presented. The mechanism which requires undissociated sulfide (6.5 M H₂SO₄) and works at temperatures close to 120 °C, proceeds at low overpotential and in the absence of hydrogen evolution. A molecular model describing the interaction of H₂SO₄ with the carbon lattice of graphite leading to the liberation of H₂S is discussed on the basis of electrochemical and photoelectron spectroscopic data. Applications of this process in energy and environmental technology (sulfide as energy source for CO₂ reducing chemoautotrophic bacteria) and for elimination of sulfuric acid waste are discussed.

Keywords: *biomass production, CO₂ reducing chemoautotrophic bacteria, graphite cathode, sulfate, sulfuric acid, thermoelectrochemical reduction*

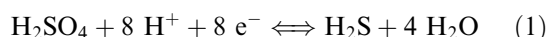
1. Introduction

Electrolytic reduction of sulfate (as H₂SO₄) to H₂S and its precipitation as a nonhazardous metal sulfide is a possible means of eliminating sulfuric acid waste. A further potential application is to provide the sulfide as energy carrier to sulfide oxidizing chemoautotrophic bacteria (*Thiobacillus ferrooxidans*) in order to convert CO₂ and H₂O to biomass (carbohydrates, proteins, lipids) via the Calvin Cycle [1]. In this process the reformed sulfate is recycled using photovoltaic electricity and solar heat for the reduction process.

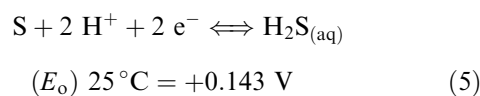
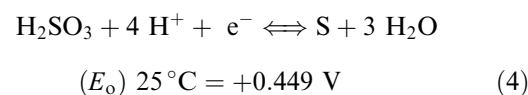
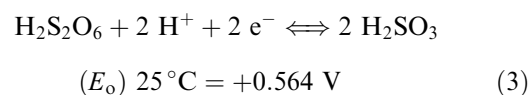
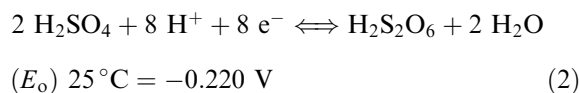
Up to now, aside from reduction via chemical reactions (e.g. reduction by means of Fe²⁺ in acid solution) or biomimetic reduction [2], only a thermal reduction of H₂SO₄ at about 1000 °C is known. The liberation of H₂S and S, observed long ago, along with H₂ during the electrolysis of concentrated H₂SO₄ using a Pt cathode [3–6], is not due to a direct electrochemical reduction of the H₂SO₄ but very probably due to the reduction by means of the hydrogen in the atomic state liberated from water splitting. This fact has been confirmed in this work as shown later.

Massive reduction of sulfate to sulfide takes place in geological environments, especially in geothermally active regions along ocean ridges where sulfate containing seawater enters the heated ocean floor and sulfide is emitted via so called ‘black smokers’, which are the energy source of a very dynamic biomass system, mediated by sulfide oxidizing and archaeobacteria.

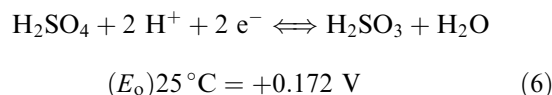
A direct electrochemical reduction of sulfate to H₂S in aqueous solution can be described according to the overall reaction



Since such an 8 e⁻-transition process is very unlikely to occur, the following reaction steps most probably take place:

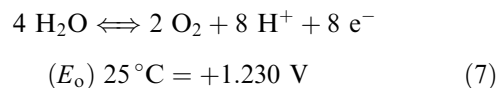


A one step reduction of H₂SO₄ to H₂SO₃ may also be considered according to



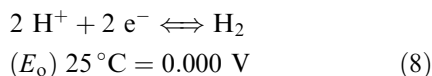
In cyclic voltammetric experiments using a RuS₂ single crystal as a working electrode [10], peaks have been found which indicate the occurrence of Reactions 4, 5 and 6.

On the anodic side, where the main reaction



takes place, other reactions can also occur which lead to the production of O₃, H₂O₂, SO₃²⁻ and S₂O₈²⁻, depending on the concentration of H₂SO₄, the tem-

perature, the electrode material and the current density. The standard potential of Reaction 7 is the thermodynamic value of the voltage of water splitting under standard conditions, since the standard potential of the reaction



is by definition zero. Only the part of the overvoltage needed for water splitting depends on the pH, since both anodic and cathodic standard potentials for water splitting depend in the same manner on pH.

Equations 2–6 show that the reduction is favoured by acid solution. At such low pH, the standard potentials of Reactions 4, 5 and 6 are within the stability range of water (E_o)_H/pH diagram). Thus the electrochemical reduction of sulfate in aqueous solution is thermodynamically possible. The fact that such reduction has not been demonstrated up to now indicates that the sulfate reduction is apparently kinetically inhibited and needs high overvoltage to take place.

The largest component of the overvoltage is due to the inhibited charge transfer from the electrode surface to the sulfate in solution, depending on the electrode material, the temperature, the current density and the physical and chemical conditions of the H_2SO_4 , particularly the degree of association between H^+ and SO_4^{2-} which influences the electron distribution along the S–O bond. In this work, the conditions for a decrease of the activation energy for the reduction process were examined.

2. Experimental details

Figure 1 shows the apparatus used for the electrochemical reduction of sulfate. It consists of a glass U-tube (dia. 30 mm, height 250 mm) whose tops are tightly fitted to refluxes, electrodes and thermometers. The electrolyte solution was blanketed by a moderately flowing air stream moving the gases produced at the electrodes from the cell atmosphere; gases produced at the cathode were passed into lead acetate (or copper sulfate) solution allowing quantitative precipitation of the sulfide produced. A spiral-shaped platinum wire of 1 mm in diameter and 400 mm in length was used as the anode. Apart from a graphite cathode (a block with the surface $F = 18.2 \text{ cm}^2$ which was connected tightly at its cylindrical top above the electrolyte surface with a Pt wire), similar spirals of Pt, Ag and Cu were also used as cathode in test experiments. H_2SO_4 solutions of different concentrations, up to 10 M, as well as aqueous Na_2SO_4 (1 M, pH 0, adjusted with H_2SO_4) and molten $\text{Na}_2\text{SO}_4(\text{H}_2\text{O})_{10}$ (melting point, 30°C) were used as electrolytes. Electrolyte temperatures up to 145°C were used using a 300 W reflector lamp. The voltage was successively increased from 0.6 up to 2.5 V. The interaction of the H_2SO_4 with the surface of the graphite electrode was investigated by means of photoelectron spectroscopy.

The generation of H_2S and its use for CO_2 -fixation was tested by precipitating H_2S and Cu^{2+} solution and by cultivating *Thiobacillus ferrooxidans* on the resulting CuS precipitate.

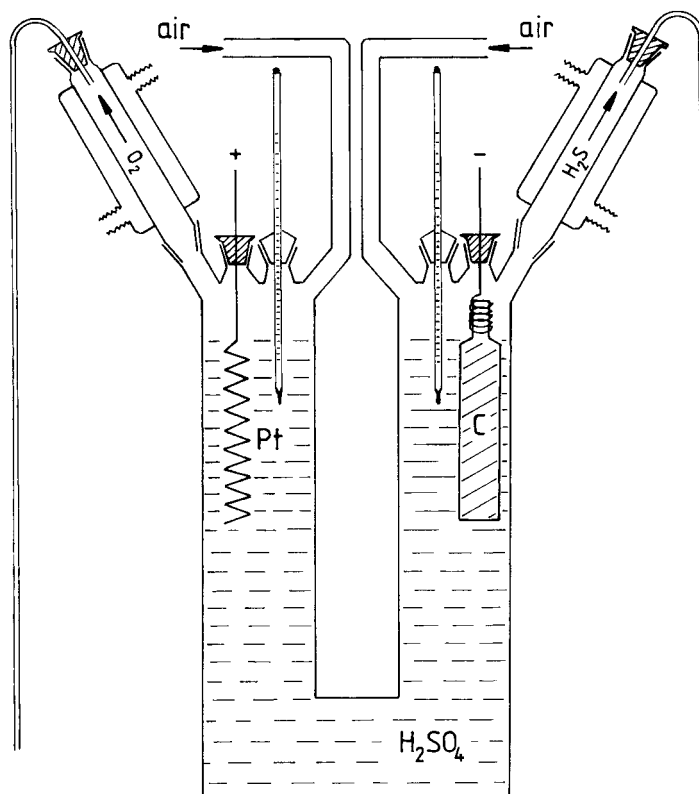


Fig. 1. Apparatus for electrolytic reduction of H_2SO_4 .

3. Results

In aqueous Na_2SO_4 solution (pH 0), and also in molten $\text{Na}_2\text{SO}_4(\text{H}_2\text{O})_{10}$, no reduction of sulfate was obtained at any of the cathode materials mentioned above, even at temperatures up to 145°C , and $U = 2.5\text{V}$. The results of the H_2SO_4 reduction are summarized in Table 1. Fig. 2 shows those obtained using a graphite cathode.

Ag and Cu, which have a relatively high hydrogen overvoltage, reacted with concentrated H_2SO_4 at about 145°C to form SO_2 which is easily reduced to H_2S , forming Ag_2S as well as CuS . At moderate H_2SO_4 concentrations around 6M and the corresponding boiling temperature, no reduction was observed even at a voltage $U = 2.5\text{V}$. In the case of Pt as cathode, formation of H_2S was only observed after water splitting (H_2 -evolution) took place.

3.1. Graphite cathode

A direct electrochemical reduction of sulfate with liberation of traces of H_2S was already obtained at $C_{\text{H}_2\text{SO}_4} = 5\text{M}$, boiling temperature (113°C) and a voltage lower than that of water splitting. At higher

H_2SO_4 concentration (6.7M), traces of H_2S were already detected at $U = 0.6\text{V}$ at 116°C as well as at boiling temperature (121°C). The limiting current of the equipment used ($36\mu\text{A}$) was too low for a possible quantitative determination as PbS in reasonable time. It is difficult to predict the thermodynamic limit of the voltage necessary for the reduction at such conditions of temperature and concentration, since neither the partial molar entropy nor the overvoltage of Reactions 6, 4 and 5 are known as functions of these conditions. However, the relatively low values of the standard potentials of these reactions, explain that the reduction at 0.6V (or perhaps even less) is possible. The liberation at $U = 1.5\text{V}$ (still much lower than that of water splitting observed at $U = 1.9\text{V}$) of H_2S became much stronger. The current efficiency (fraction of the current liberating H_2S and quantitatively determined as PbS) increased drastically with increasing temperature: 1% at 102°C and current density $i = 0.025\text{mA cm}^{-2}$, 45% at 116°C , $i = 0.20\text{mA cm}^{-2}$ and 60% at 121°C , $i = 0.017\text{mA cm}^{-2}$. At 1.9V , efficiency maximum of 2% at 102°C , $i = 0.17\text{mA cm}^{-2}$, 58% at 116°C , $i = 0.151\text{mA cm}^{-2}$ and 80% at 121°C , $i = 0.147\text{mA cm}^{-2}$. These results clearly show that a

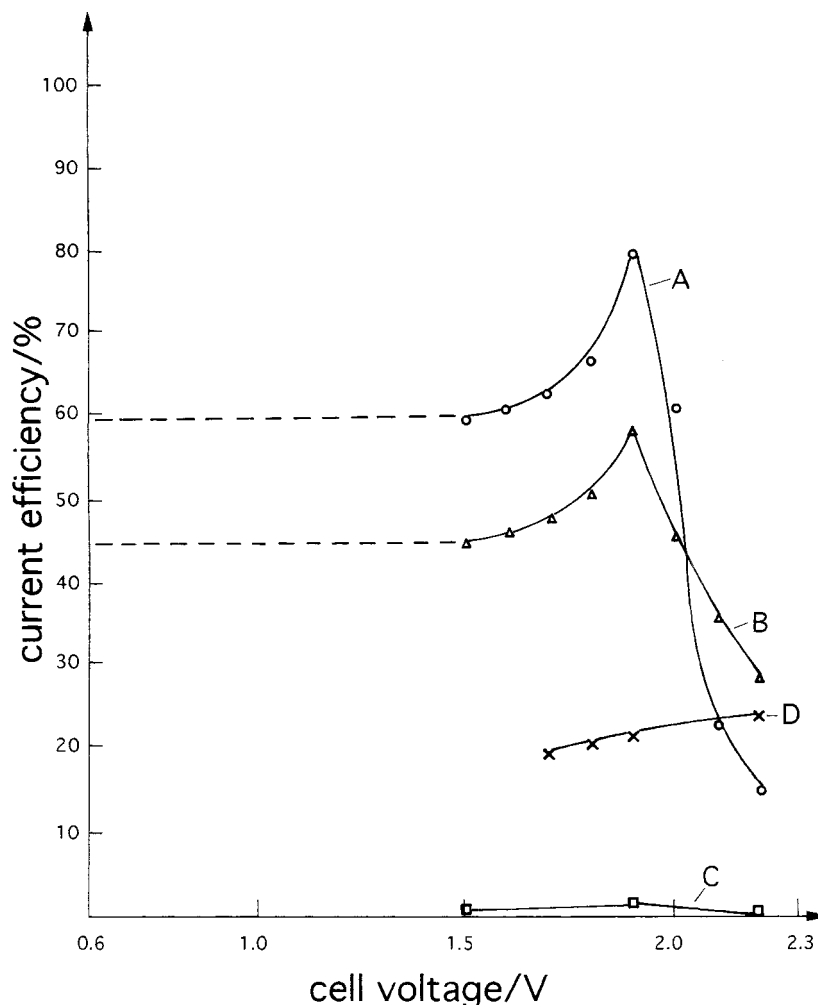


Fig. 2. Current efficiency of the reduction of H_2SO_4 at graphite cathode as a function of cell voltage: (curve A: 6.7M , 121°C), (curve B: 6.7M , 116°C), (curve C: 6.7M , 102°C) and (curve D: 9.7M , 145°C).

Table 1. Results of the reduction of H_2SO_4

| <i>Expt.</i> | $C_{H_2SO_4}$ /M | <i>Cathode</i> | <i>T</i> /°C | <i>U</i> /V | <i>i</i> /mA cm ⁻² | <i>Current efficiency</i> /% converted to H ₂ S | <i>Remarks</i> |
|--------------|---------------------|----------------|-----------------|-------------------|----------------------------------|------------------------------------------------------------------|--------------------------------------------------------------------------------------------------------------------------------------------------------------------------------------------------------|
| (1) | 5 | Pt | 113 | 1.8–2.2 | 0.14–3.32 | – | No formation of H ₂ S, only water splitting |
| (2) | 5 | C | 113 | 1.8 | 0.13 | H ₂ S-traces | Still no water splitting, but traces of H ₂ S were detected with Pb (CH ₃ COO) ₂ paper |
| | | | | 1.9–2.2 | 0.23–2.29 H ₂ | S-traces | Traces of H ₂ S before water splitting at 1.9 V |
| (3) | 6.7 | Pt | 121 | 1.9–2.11 2.2 | 0.21–1.23 2.11 | – H ₂ S-traces | No formation of H ₂ S, but water splitting. Traces of H ₂ S were observed |
| (4) | 6.7 | C | 102 | 1.5 1.9 2.2 | 0.025 0.17 1.67 | 1 2 0.5 | Direct reduction before water splitting took place at 1.9 V. The yield decrease between 1.99 and 2.2 V is due to the consumption of current, mainly in water splitting |
| (5) | 6.7 | C | 116 | 0.6 | (2 μA cm ⁻²) | | Direct reduction, but only traces of H ₂ S could be detected with Pb (CH ₃ COO) ₂ paper. Because of very low current used, no quantitative determination was possible |
| | | | | 1.5 | 0.20 | 45 | Direct reduction before water splitting |
| | | | | 1.6 | 0.027 | 46.5 | occurred around 1.9 V, |
| | | | | 1.7 | 0.057 | 48 | where a yield |
| | | | | 1.8 | 0.080 | 51 | maximum is obtained. |
| | | | | 1.9 | 0.151 | 58 | Yield decrease at |
| | | | | 2.0 | 0.252 | 46 | $U > 1.9$ V due to the |
| | | | | 2.1 | 0.895 | 36 | same reason as in expt. 4 |
| | | | | 2.2 | 1.452 | 29 | The same observation as in expt. 5 |
| (6) | 6.7 | C | 121 | 0.6 | (1.95 μA cm ⁻²) | | Higher yield at 1.5 and 1.9 V due to the higher temperature, but lower yield at $U = 2.0$ – 2.2 V very probably due |
| | | | | 1.5 | 0.017 | 60 | higher rate of water splitting |
| | | | | 1.6 | 0.024 | 61 | |
| | | | | 1.7 | 0.055 | 63 | |
| | | | | 1.8 | 0.076 | 67 | |
| | | | | 1.9 | 0.147 | 80 | |
| | | | | 2.0 | 0.247 | 61 | |
| | | | | 2.1 | 0.846 | 23 | |
| | | | | 2.2 | 1.456 | 15 | |
| (7) | 9.7 | C | 145 | 1.7 | 0.056 | 20 | The yield of H ₂ S is much lower than in expts 5 and 6, because of the formation of sulfur which was observed at the cathode. |
| | | | | 1.8 | 0.075 | 21 | |
| | | | | 1.9 | 0.148 | 22 | |
| | | | | 2.2 | 1.46 | 24.5 | |
| (8) | 9.7 | Pt | 145 | 1.9–2.1 | 0.22–1.24 | H ₂ S _x ? | Probably H ₂ S _x was formed, since a black yellow precipitate was obtained in Pb (CH ₃ COO) ₂ solution. |
| | | | | 2.2 | 2.10 | 24 | PbS is obtained in Pb (CH ₃ COO) ₂ solution and sulfur was formed at the cathode |

higher current efficiency is obtained at high temperature (higher degree of association between SO_4^{2-} and H^+ , parallel with a significant decrease in the dielectric constant of water with increasing temperature), but not as a consequence of the current density, which varied slightly in the opposite direction due to the decreasing dissociation of the sulfuric acid.

The extrapolation of curves A and B in Fig. 2 shows that probably the same current efficiency, such as found at 1.5 V, could also be obtained at a cell voltage of 0.6 V if a much bigger electrode surface were used to give a sufficiently high current to make a quantitative determination possible in reasonable time. At $U > 1.9$ V a drastic decrease in current efficiency was observed, which is due to the rising fraction of the current consumed in water splitting. Curve A in Fig. 2 descends more rapidly than curve B, probably due to the higher part of the current consumed in water splitting at 121 °C than at 116 °C. This explains the crossing of the curves around $U = 2.03$ V.

At higher H_2SO_4 concentration (9.7 M) and boiling temperature (145 °C), and nearly the same current densities as in the case of reduction of 6.7 M H_2SO_4 at 121 °C, the current efficiency (even at lower voltage than that of water splitting) is much lower than that obtained in the case of 6.7 M H_2SO_4 despite similar current densities. This decrease is due to the competing reduction to sulfur which was observed in the cathode chamber. However, the efficiency curve increased slightly from 20% at $U = 1.7$ V and $i = 0.056$ mA cm⁻², 22% at $U = 1.9$ V and $i = 0.148$ mA cm⁻², to 24.5% at $U = 2.2$ V and $i = 1.46$ mA cm⁻² and seems to remain unchanged at higher voltage and current density. This behaviour was unexpected in comparison with that for 6.7 M H_2SO_4 , since it is unlikely that the different parts of the current consumed in the production of H_2S , sulfur and water splitting (including the entropy term) remain more or less the same with increasing voltage and current density. More detailed experiments, including a quantitative determination of the sulfur and the hydrogen must be carried out to get this point clear.

As an additional test for the liberation of H_2S during cathodic reduction of H_2SO_4 on graphite, and in order to demonstrate its relevance for an energy cycle based on sulfur, H_2S was precipitated with Cu^{2+} to give CuS . *Thiobacillus ferrooxidans* was cultivated on this sulfide as the only energy source and bacterial growth was clearly verified.

3.2. Pt cathode

Up to 2.2 V and $i = 3.32$ mA cm⁻², no formation of H_2S , but only water splitting, was observed in 5 M H_2SO_4 at boiling temperature (113 °C). Also, 6.7 M H_2SO_4 , 121 °C, U up to 2.1 V and $i = 1.23$ mA cm⁻², no formation of H_2S took place. Starting at $U = 2.2$ V and $i = 2.11$ mA cm⁻², traces of H_2S were detected. In 9.7 M H_2SO_4 , 145 °C, $U = 1.9$ V and

$i = 0.22$ mA cm⁻², very probably a reduction to H_2S and sulfur by means of hydrogen arising from water splitting occurred, since the gas products passed into $\text{Pb}(\text{CH}_3\text{COO})_2$ solution gave a black yellow precipitate which was partially soluble in CS_2 . At $U = 2.2$ V and $i = 2.10$ mA cm⁻² the reduction accompanying the stronger water splitting led to the formation of H_2S but only with a current efficiency of 24%.

The photoelectron spectra of a reference graphite without any contact with H_2SO_4 are shown in Figs. 3A(a), 3B(a), 3C(a) and 4(a). Those of a graphite electrode, after running the reduction experiments, are shown in Figs. 3A(b), 3B(b), 3C(b) and 4(b). Fig. 3A(b) shows the S^{2p} peak at 168.8 eV which refers to sulfur coordinated with 4 O-atoms in sulfate. No signal is observed in Fig. 3A(a). Also the oxygen spectrum O^{1s} in Fig. 3B(b) clearly shows the peak at 531.8 eV referring to the oxygen bond in sulfate, whereas the very flat peak in Fig. 3B(a), which is shifted to higher energy and refers to a C–O bond, is apparently due to interaction with the atmospheric oxygen (the samples were heated). The C^{1s} spectrum in Fig. 3C(b) shows a peak which is shifted to lower energy and is of much lower intensity in comparison to the peak in Fig. 3C(a). This confirms that the C-atoms at the surface of the graphite electrode are not only bonded to neighbouring C-atoms in the graphite lattice, but also to other atoms. Spectrum 3C(b) shows, furthermore, a shoulder at an energy of about 286 eV which corresponds to a C–S bond and is very probably due to a weak interaction of the unpaired electrons in the C-atoms with the S-atoms in sulfate. Curves 4(a) and 4(b), which are normalized to the same current, show this aspect more clearly.

4. Discussion

4.1. Electrode material

Except for Pt, the materials used as cathodes have a relatively high hydrogen overvoltage in order to suppress the competing hydrogen evolution Reaction 8. Graphite is a material which is, moreover, corrosion resistant (denoted below as C). The layer structure of this material shows hexagonal C-rings with conjugated π -bonds and therefore has a conduction band with delocalized electrons. It offers the interesting possibility that H_2SO_4 forms an intermediate compound $\text{C}_m \cdot x \text{H}_2\text{SO}_4$ in which the S–O of the sulfate may be conjugated with the double π -bond system of the hexagonal C-rings in the layers. This compound may have a lower activation energy of reduction due to easier charge transfer from the conduction level in graphite to sulfate.

4.2. Effect of temperature, pressure and concentration

Electron transfer to sulfate is assumed to take place more easily when the two negative charges of the free ion are neutralized by means of positive ligands which

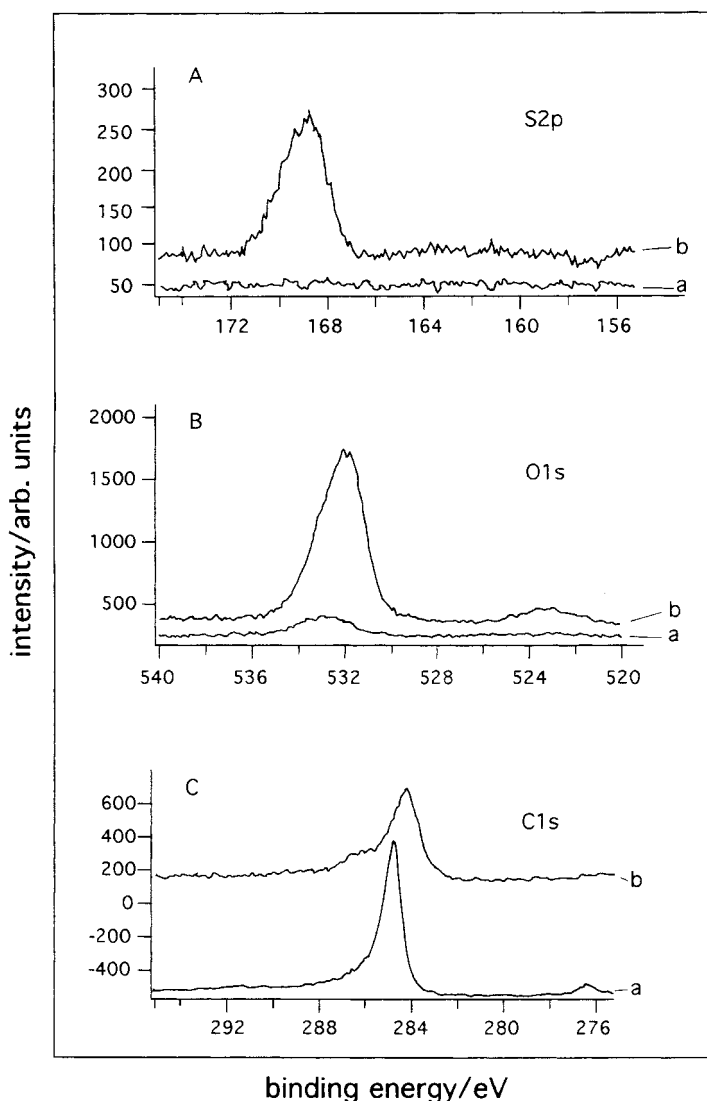


Fig. 3. (A) Photoelectron spectrum (S^{2p}) in a reference graphite (3A(a)) and in the used graphite electrode (3A(b)). (B) Photoelectron spectrum (O^{1s}) in a reference graphite (3B(a)) and in the used electrode (3B,b). (C) Photoelectron spectrum (C^{1s}) in a reference graphite (3C(a)) and in the used graphite electrode (3C(b)).

are electrostatically or covalently bonded to the oxygen. The so caused polarization of the S–O-bond shifts the electron density away from the S-atom. Such decrease in the electron density around the S-atom could easily be obtained using protons as positive ligands to from undissociated H_2SO_4 . The dissociation of sulfuric acid is rapidly suppressed with increasing temperature and concentration [7, 8]. Higher temperature not only supplies at least a part of the necessary activation energy, but also leads to a drastically increased association between SO_4^{2-} and H^+ . Since the degree of dissociation of H_2SO_4 at constant temperature and given sulfate concentration increases with increasing pressure [7, 8] and, in addition, reactions giving gas products are hindered by pressure increase, no catalytic effect of pressure was expected.

The results obtained confirm the above hypothesis, namely that

- (i) direct reduction of H_2SO_4 is only possible when the acid is highly undissociated at conditions of fairly high temperature (optimum: 121 °C) and

moderately high concentration (optimum: 6.7 M) and

- (ii) the obviously high activation energy needed for a direct reduction to occur can be drastically reduced when a suitable cathode material such as graphite is used.

Figures 5(a)–(f) show a proposed mechanism of the reduction of the H_2SO_4 intermediary bonded between the graphite layers. The tetrahedrally structured H_2SO_4 has four σ bonds and 2 $d_{\pi-p\pi}$ S–O-bonds (Fig. 5(a.1)). The C-atoms at the end of two neighbouring graphite layers have unpaired electrons (Fig. 5(a.2)). Because of the higher energy of the $d_{\pi-p\pi}$ -bond in comparison to the σ C–O-bond, each of the unpaired electrons of the two C-atoms is paired with one electron of each of the O-atoms having the $d_{\pi-p\pi}$ -bond to form 2 σ C–O-bonds with optimum orbital overlapping and two electrons are set free at the S-atom (Fig. 5(a.3)).

The second step is assumed to be a charge transfer from the 2 σ O–S-bonds to the

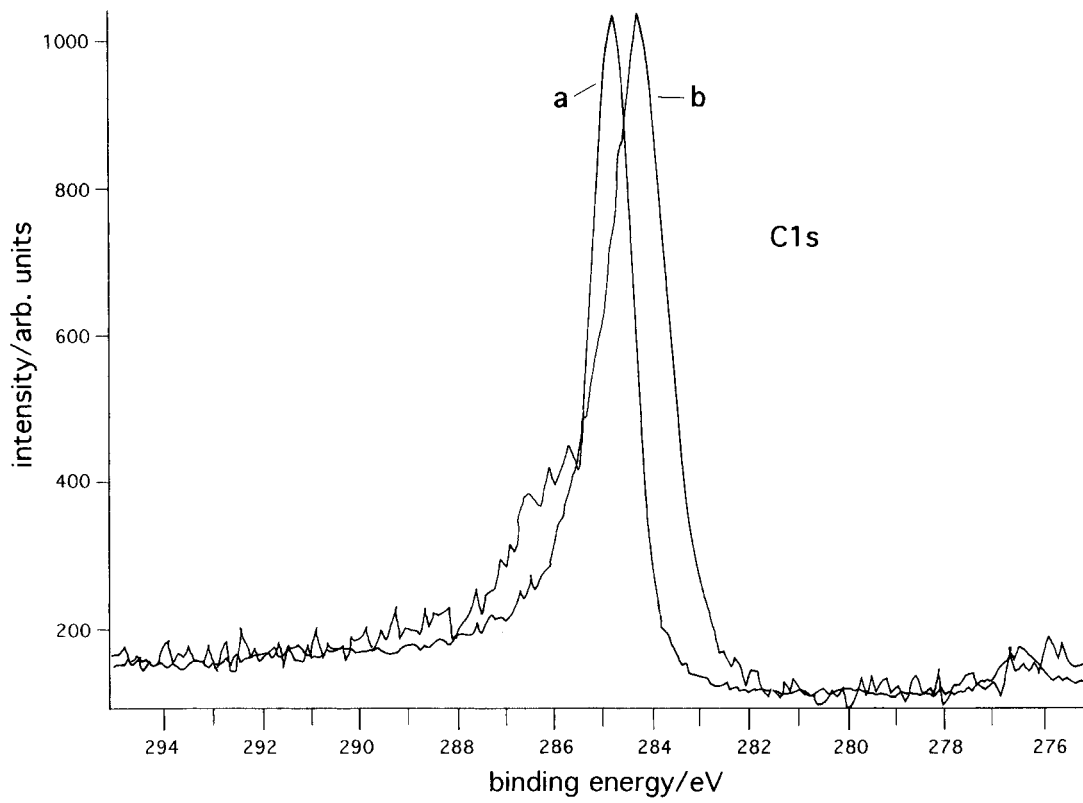


Fig. 4. Spectrum of Fig. 3C, normalized to the same intensity.

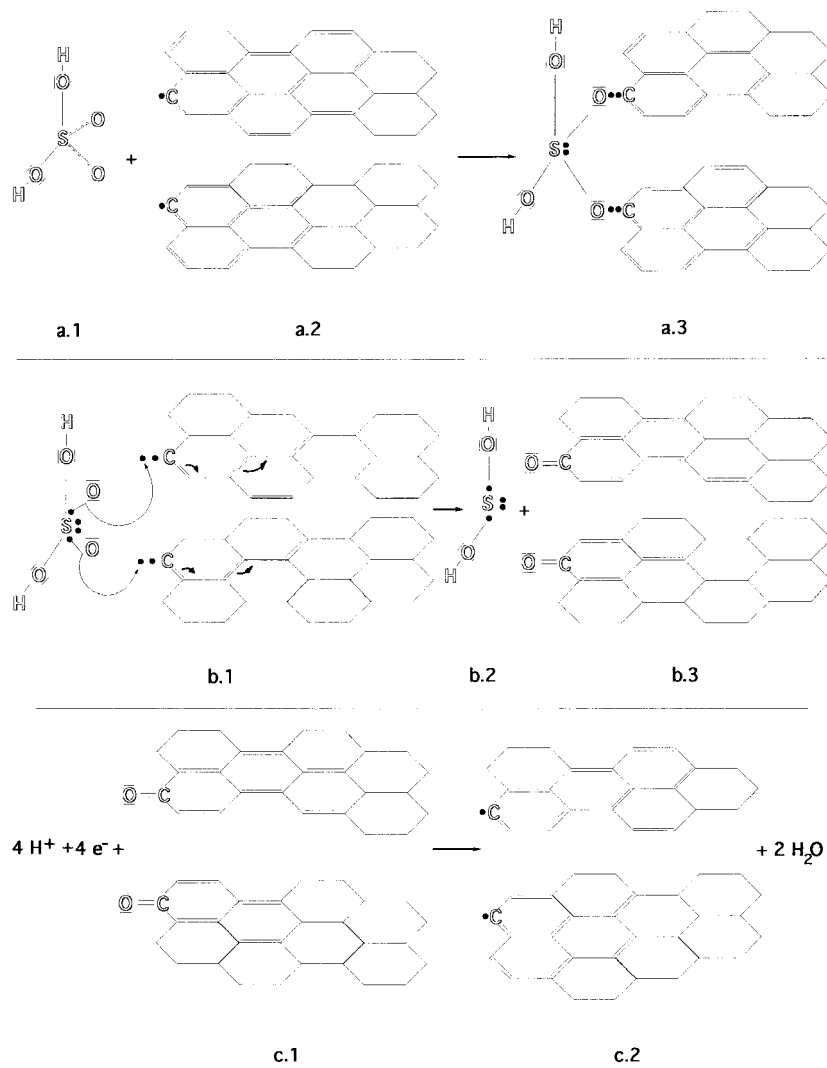


Fig. 5.

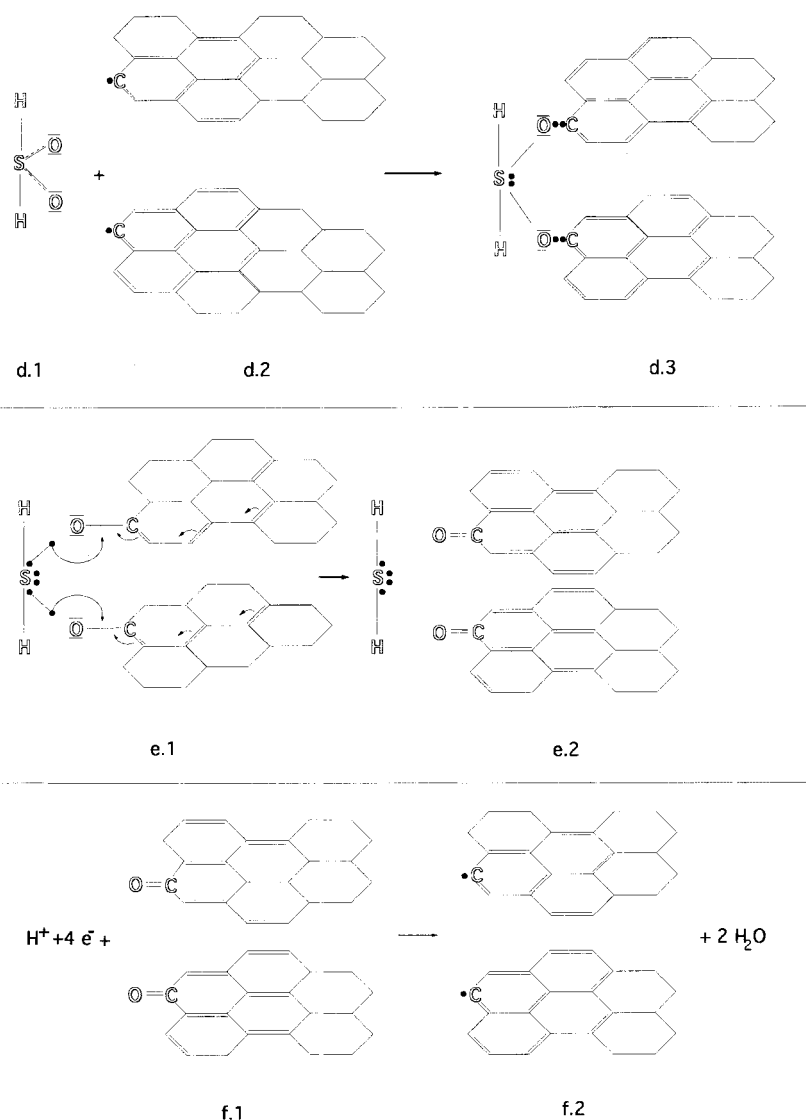


Fig. 5. Postulated mechanism of H_2SO_4 reduction at graphite cathode.

two C-atoms (Fig. 5(b.1)), where a simultaneous rearrangement of the conjugation system occurs in order to form the energetically more stable system with two ketone bonds conjugated with the double bonds of the C-rings in the layers (Fig. 5(b.3)). H_2SO_4 is hereby reduced to $\text{H}_2\text{O}_2\text{S}$ (sulfoxylic acid) with two electron pairs at the S-atom (Fig. 5(b.2)).

The third step is assumed to be the reduction of the ketone groups to obtain the original form of the graphite layers with C-atoms having unpaired electrons and water as shown in (Fig. 5(c.1)) and (Fig. 5(c.2)).

As fourth step it is proposed that the two O-atoms of the tautomeric form (Fig. 5(d.1)) of the sulfoxylic acid (in which the S-atom has a σ -bond with each of the two H-atoms, one σ -bond and one d-p-bond with each of the two O-atoms) are again bonded to the original graphite form in (Fig. 5(d.2)) and the same procedure as in the steps before [(Fig. 5(d.1)) + (Fig. 5(d.2)) \rightarrow (Fig. 5(d.3)), Fig. 5(e.1) \rightarrow H_2S + (Fig. 5(e.2)) and (Fig. 5(f.1)) + $4\text{H}^+ + 4\text{e}^- \rightarrow$ (Fig. 5(f.2)) + $2\text{H}_2\text{O}$] takes place.

The XPS-measurements appear to be consistent with this model, especially in that they demonstrate a chemical change of the carbon environment, and the presence of sulfur and oxygen in a sulfate environment. The evidence of sulfur-carbon interaction (286 eV), which appears as a shoulder in Fig. 4(b), suggests that we are dealing with a partial interfacial intercalation of the sulfur species during the catalytic reduction process where neighbouring carbon sheets can participate in the chemical interaction.

5. Applications

5.1. Elimination of sulfuric acid waste

Sulfuric acid waste arises in many chemical processes. Up to now, the only ways used for its disposal is its environmental harmful release into the sea or conversion at high temperature (1000°C). By means of the above described electrolytic reduction, it is possible to convert the acid to nonhazardous sulfide via simple technology. Taking the data for the maximum current efficiency in experiment 6, Table 1 (6.7 M

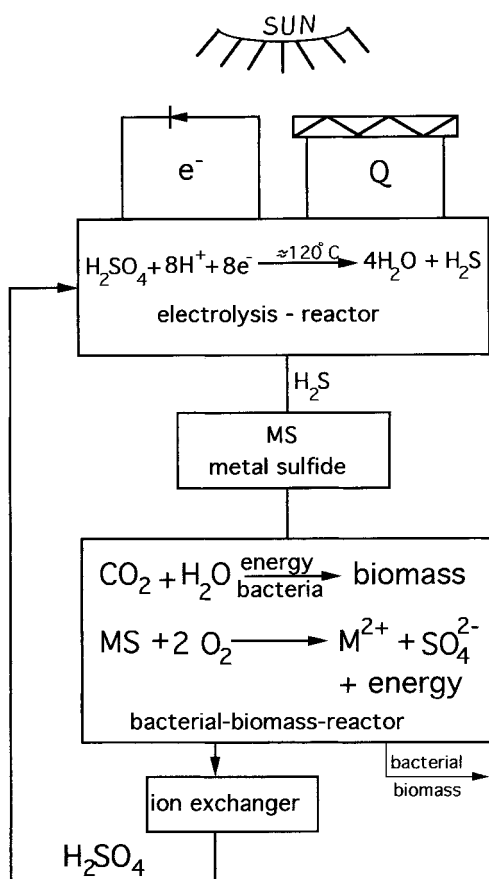


Fig. 6. Diagram of solar powered biomass production process based on thermoelectrochemical reduction of sulfate to sulfide.

H_2SO_4 , graphite cathode, $T = 121^\circ C$, $U = 1.9 V$, $i = 0.147 mA cm^{-2}$ and current efficiency 80%), 1 kWh is required for reduction of 1.97 mol sulfuric acid to H_2S .

5.2. Solar powered bacterial biomass production

Figure 6 shows a diagram of a solar powered bacterial production process which could be run even in

arid areas where no plant photosynthesis is possible. Temperatures around $120^\circ C$, necessary for the electrocatalytic reduction of H_2SO_4 (around 6.5 M) to H_2S for the graphite cathode, could be easily obtained using a solar thermal collector and the electric energy may be generated by photovoltaic panels. The energy carrier H_2S is precipitated as metal sulfide which is fed to CO_2 reducing bacteria (*Thiobacillus ferrooxidans*) to convert it, in the presence of oxygen and water, to biomass (carbohydrates, proteins, lipids) according to the Calvin cycle, where it is re-oxidized to SO_4^{2-} (process verified during this work). After separation of the biomass, the sulfate is separated as H_2SO_4 by means of anion exchange and recycled for re-reduction (Fig. 6). A detailed description of the sulfate reduction as part of a biomass producing solar powered fuel cycle is given elsewhere [9].

Acknowledgements

The authors gratefully acknowledge the assistance of E. Mueller in performing the electrochemical experiments, and thank H. Sehnert for carrying out the XPS-measurements and J. Rojas-Chapana for performing the experiments with *Thiobacillus ferrooxidans*.

References

- [1] H. Tributsch, *Nature* **281** (1979) 555.
- [2] O. A. E. Shigeru and Hideo Togo, *Bull. Chem. Soc. Jpn.* **56** (1983) 3828.
- [3] E. Gehrcke, *Verh. Phys. Ges.* **5** (1903) 263.
- [4] C. G. Schluederberg, *J. Phys. Chem.* **12** (1908) 574.
- [5] W. D. Brandcroft and J. E. Magoffin, *J. Am. Soc.* **57** (1935) 2561.
- [6] H. Hoffmann, *Z. Elektroch.* **27** (1921) 442.
- [7] B. A. Bilal and E. Müller, *Z. Naturforsch.* **48a** (1993) 1073.
- [8] *Idem, Ibid.* **49a** (1994) 939.
- [9] B. A. Bilal and H. Tributsch, *J. Chem. Technol. Biotechnol.* to be published.